

Extracting the Locus of Attention at a Cocktail Party from Single-Trial EEG using a Joint CNN-LSTM Model

Ivine Kuruvila¹, Jan Muncke¹, Eghart Fischer², Ulrich Hoppe¹

Abstract—Human brain performs remarkably well in segregating a particular speaker from interfering speakers in a multi-speaker scenario. It has been recently shown that we can quantitatively evaluate the segregation capability by modelling the relationship between the speech signals present in an auditory scene and the cortical signals of the listener measured using electroencephalography (EEG). This has opened up avenues to integrate neuro-feedback into hearing aids whereby the device can infer user’s attention and enhance the attended speaker. Commonly used algorithms to infer the auditory attention are based on linear systems theory where the speech cues such as envelopes are mapped on to the EEG signals. Here, we present a joint convolutional neural network (CNN) - long short-term memory (LSTM) model to infer the auditory attention. Our joint CNN-LSTM model takes the EEG signals and the spectrogram of the multiple speakers as inputs and classifies the attention to one of the speakers. We evaluated the reliability of our neural network using three different datasets comprising of 61 subjects where, each subject undertook a dual-speaker experiment. The three datasets analysed corresponded to speech stimuli presented in three different languages namely German, Danish and Dutch. Using the proposed joint CNN-LSTM model, we obtained a median decoding accuracy of 77.2% at a trial duration of three seconds. Furthermore, we evaluated the amount of sparsity that our model can tolerate by means of magnitude pruning and found that the model can tolerate up to 50% sparsity without substantial loss of decoding accuracy.

I. INTRODUCTION

Holding a conversation in presence of multiple noise sources and interfering speakers is a task that people with normal hearing does exceptionally well. The inherent ability to focus the auditory attention on a particular speech signal in a complex mixture has helped us to overcome what is known as the cocktail party effect [1]. However, an automatic machine based solution to the cocktail party problem is yet to be discovered despite the intense research for more than half a century. Such a solution is highly desirable for a plethora of applications such as human-machine interface (e.g. Amazon Alexa), automatic captioning of audio/video recordings (e.g. YouTube, Netflix), advanced hearing aids etc.

In the domain of hearing aids, people with hearing loss suffer from deteriorated speech intelligibility when listening to a particular speaker in a multi-speaker scenario. Hearing aids currently available in the market often do not provide sufficient amenity in such scenarios due to their inability to distinguish between the attended speaker and the ignored

This work was carried out at the ENT clinic, Friedrich-Alexander-Universität Erlangen-Nürnberg (FAU), Erlangen, Germany.

¹Ivine Kuruvila, Jan Muncke and Ulrich Hoppe are with Department of Audiology, ENT-Clinic, Friedrich-Alexander-Universität Erlangen-Nürnberg (FAU), Erlangen, Germany. Ulrich.Hoppe@uk-erlangen.de

²Eghart Fischer is with WS Audiology, Erlangen, Germany.

speakers. Hence, additional information about the locus of attention is highly desirable. In visual domain, selective attention is explained in terms of visual object formation where an observer focuses on a certain object in a complex visual scene [2]. This was extended to auditory domain where it was suggested that phenomena such as cocktail party effect could be better understood using auditory object formation [3]. I.e., brain forms objects based on the multiple speakers present in an auditory scene and selects those objects belonging to a particular speaker during attentive listening (top-down or late selection). However, flexible locus of attention theory was concurrently proposed where the late selection is hypothesized to occur at low cognitive load and early selection is hypothesized to occur at high cognitive load [4]. This has inspired investigation into whether cortical signals can provide additional information that could help to discriminate between the attended speaker and interfering speakers. In a dual-speaker experiment, it was observed that the cortical signals measured using implanted electrodes track the salient features of the attended speaker stronger than the ignored speaker [5]. Similar results were obtained using magnetoencephalography and electroencephalography (EEG) [6] [7]. In recent years, EEG analyses have become the commonly used methodology in attention research which is lately known as auditory attention decoding (AAD).

Both low level acoustic features (speech envelope or speech spectrogram) and high level features (phonemes or phonetics) have been used to investigate the speech tracking in cortical signals [8] [9] [10] [11]. State-of-the-art AAD algorithms are based on the theory of linear systems where acoustic features are linearly mapped on to the EEG signals. This mapping can be either in the forward direction [9] [12] [13] or in the backward direction [7] [14] [15]. These algorithms have been successful in providing insights into the underlying neuroscientific processes by which brain suppresses the ignored speaker in a multi-speaker scenario. Using speech envelope as the input acoustic feature, linear algorithms could generate system response functions that characterize the auditory pathway in the forward direction. These system response functions are referred to as temporal response function (TRF) [9]. Analysis of the shape of TRFs has revealed that the human brain encodes the attended speaker and the ignored speaker differently. I.e., TRFs corresponding to the attended speaker have salient peaks around 100 ms and 200 ms which are not present in TRFs corresponding to the ignored speaker [16] [17]. Similar attention modulation effects were observed when using speech spectrogram and higher level features such as phonetics as the acoustic input [10]. Likewise, using backward models, the input stimulus can be reconstructed from EEG signals (stimulus reconstruction method) and a listener’s

Name	Number of Subjects	Duration per Subject (minutes)	Total duration (hours)	Experiment type	Language
FAU_Dataset	27	30	13.5	male + male	German
DTU_Dataset	18	50	15	male + female	Danish
KUL_Dataset	16	24	6.4	male + male	Dutch

TABLE I: *Details of the EEG datasets analysed.*

attention could be inferred by comparing the reconstructed stimulus to the input stimuli [7]. These findings give the possibility of integrating AAD algorithms into hearing aids which in combination with robust speech separation algorithms could greatly improve the amenity provided to the users.

It has been well established that the human auditory system is inherently non-linear [18] and AAD analysis based on linear systems theory addresses the issue of non-linearity to a certain extend in the preprocessing stage. For e.g., during speech envelope extraction. Another limitation of linear methods is the longer time delay required to classify attention [19] [20], although there were attempts to overcome this limitation [17] [21]. In the last few years, deep neural networks have become popular especially in the field of computer vision and speech processing. Since neural networks have the ability to model non-linearity, they have been used to estimate the dynamic state of brain from EEG signals [22]. Similarly, in AAD paradigm, convolutional neural network (CNN) based models were proposed where the stimulus reconstruction algorithm was implemented using the CNN model to infer attention [23] [24]. A direct classification of attention which bypasses the regression task of stimulus reconstruction, instead classifies whether the attention is to speaker 1 or speaker 2 directly was proposed in [24] [25]. In a non-competing speaker experiment, classifying attention as successful vs unsuccessful or match vs mismatch was further addressed in [26] [27].

All aforementioned neural network models either did not use speech features or made use of only speech envelope as the input feature. As neural networks are data driven models, additional data/information about the speech stimuli may improve the performance of the network. In neural network based speech separation algorithms, spectrogram is used as the input feature to separate multiple speakers from a speech mixture [28]. Inspired by the joint audio-visual speech separation model [29], we present a novel neural network framework that make use the speech spectrogram of multiple speakers and the EEG signals as inputs to classify the auditory attention.

The rest of the paper is organized as follows. In section II, details of the datasets that were used to train and validate the neural network are provided. In section III, the neural network architecture is explained in detail. The results are presented in section IV and section V provides a discussion of the results.

II. MATERIALS AND METHODS

A. Examined EEG datasets

We evaluated the performance of our neural network model using three different EEG datasets. The first dataset was collected at our lab and it will be referred to as FAU_Dataset [17]. The second and third datasets are publicly available and they will be referred to as DTU_Dataset [30] and KUL_Dataset [31].

1) *FAU_Dataset*: This dataset comprised of EEG collected from 27 subjects who were all native German speakers. A cocktail party effect was simulated by presenting two speech stimuli simultaneously using loudspeakers and the subject was asked to attend selectively to one of the two stimuli. Speech stimuli were taken from the slowly spoken news section of the German news website www.dw.de and were read by two male speakers. The experiment consisted of six different presentations with each presentation being approximately five minutes long making it a total of 30 minutes. EEG was collected using 21 AgCl electrodes placed over the scalp according to the 10-20 EEG format. The reference electrode was placed at the right mastoid, the ground electrode was placed at the left earlobe and the EEG signals were sampled at 2500 Hz. More details of the experiment could be found in [17].

2) *DTU_Dataset*: This is a publicly available dataset that was part of the work presented in [19]. The dataset consisted of 18 subjects who selectively attended to one of the two simultaneous speakers. Speech stimuli were excerpts taken from Danish audiobooks that were narrated by a male and a female speaker. The experiment consisted of 60 segments with each segment being 50 seconds long making it a total of 50 minutes. EEG were recorded using 64 electrodes and were sampled at 512 Hz. The reference electrode was chosen either as the left mastoid or as the right mastoid after visual inspection. Further details can be found in [19] [30].

3) *KUL_Dataset*: The final dataset that was analysed is another publicly available dataset where 16 subjects undertook selective attention experiment. Speech stimuli consisted of four Dutch stories narrated by male speakers. Each story was 12 minutes long which was further divided into two 6-minutes presentations. EEG was recorded using 64 electrodes and were sampled at 8196 Hz. The reference electrode was chosen either as TP7 or as TP8 electrode after visually inspecting the quality of the EEG signal measured at these locations. The experiment consisted of three different conditions namely HRTF, dichotic and repeated stimuli. In this work, we analysed only the

dichotic condition which was 24 minutes long. Additional details about the experiment and the dataset can be found in [31] [32].

Details of the datasets are summarized again in Table I. A total of 34.9 hours of EEG data were examined in this work. However, the speech stimuli used were identical across subjects per dataset and they totaled 104 minutes of dual-speaker data. For each subject, the training and the test data were split as 75% - 25% and we ensured that no part of the EEG or the speech used in the test data was part of the training data. The test data were further divided equally into two halves and one half was used as a validation set during the training process.

B. Data Analysis

As EEG signals analysed were collected at different sampling frequencies, they were all low pass filtered at a cut off frequency of 32 Hz and downsampled to 64 Hz sampling rate. Additionally, signals measured at only 10 electrode locations were considered for analysis and they were F7, F3, F4, F8, T7, C3, Cz, C4, T8, Pz. We analysed four different trial durations in this study namely two seconds, three seconds, four seconds and five seconds. For 2 seconds trials, an overlap of one second was applied. Thus, there were 118922 trials in total for analysis. In order to maintain the total number of trials constant, two seconds of overlap was used in case of 3 seconds trial, three seconds of overlap was used in case of 4 seconds trial and four seconds overlap was used in case of 5 seconds trial. EEG signals in each trial were further high pass filtered with a cut off frequency of 1 Hz and the filtered signals were normalized to have zero mean and unit variance at each electrode location.

Trial duration (sec)	EEG data (time x num_electrodes)	Speech data (time x freq)
2	128x10	101x257
3	192x10	151x257
4	256x10	201x257
5	320x10	251x257

TABLE II: Trial duration vs dimension of the input

Speech stimuli were initially low pass filtered with a cut off frequency of 8 kHz and were downsampled to a sampling rate of 16 kHz. Subsequently, they were segmented into trials with a duration of two seconds, three seconds, four seconds and five seconds at an overlap of one, two, three and four seconds respectively. The speech spectrogram for each trial was obtained by taking the absolute value of the short-time Fourier transform (STFT) coefficients. The STFT was computed using a Hann window of 32 ms duration with a 12 ms overlap. Most of the analysis in our work were performed using 3 seconds trial and other trial durations were used only for comparison purposes. A summary of the dimensions of EEG signals and speech spectrogram after preprocessing for different trial durations is provided in Table II.

III. NETWORK ARCHITECTURE

A top level view of the proposed neural network architecture is shown in Fig.1. It consists of three subnetworks namely EEG_CNN, Audio_CNN and AE_Concat.

A. EEG_CNN

The EEG subnetwork comprised of four different convolutional layers as shown in Table III. The kernel size of the first layer was chosen as 24 and it corresponded to a latency of 375 ms in the time domain. A longer kernel was chosen because previous studies have shown that the TRFs corresponding to the attended and unattended speakers differ around 100 ms and 200 ms [16] [17]. Therefore, a latency of 375 ms could help us to extract features that modulate the attention to different speakers in a multi-speaker environment. All other layers were initialized with kernels of shorter duration as shown in Table III. All convolutions were performed using a stride of 1x1 and after the convolutions, max pooling was used to reduce the dimensionality. To prevent overfitting on the training data and improve generalization, dropout [33] and batch normalization (BN) [34] were applied. Subsequently, the output was passed through a non-linear activation function which was chosen as rectified linear unit (ReLU). The dimension of the input to EEG_CNN varied according to the length of the trial (Table II) but the dimension of the output was fixed at 48x32. The max pooling parameter was slightly modified for different trial durations to obtain the fixed output dimension. The first dimension (48) corresponded to the temporal axis and the second dimension (32) corresponded to the number of convolution kernels. The dimension of the output that mapped the EEG signals measured at different electrodes was reduced to one by the successive application of max pooling along the electrode axis.

	Number of Kernels	Kernel Size	Dilation	Padding	Maxpool
Layer 1	32	24x1	1,1	12,0	2,1
Layer 2	32	7x1	2,1	6,0	1,2
Layer 3	32	7x5	1,1	3,2	2,5
Layer 4	32	7x1	1,1	3,0	1,1

TABLE III: CNN parameters of the EEG subnetwork

	Number of Kernels	Kernel Size	Dilation	Padding	Maxpool
Layer 1	32	1x7	1,1	0,3	1,1
Layer 2	32	7x1	1,1	0,0	1,4
Layer 3	32	3x5	8,8	0,16	1,2
Layer 4	32	3,3	16,16	0,16	1,1
Layer 5	1	1x1	1,1	0,0	2,2

TABLE IV: CNN parameters of the Audio subnetwork

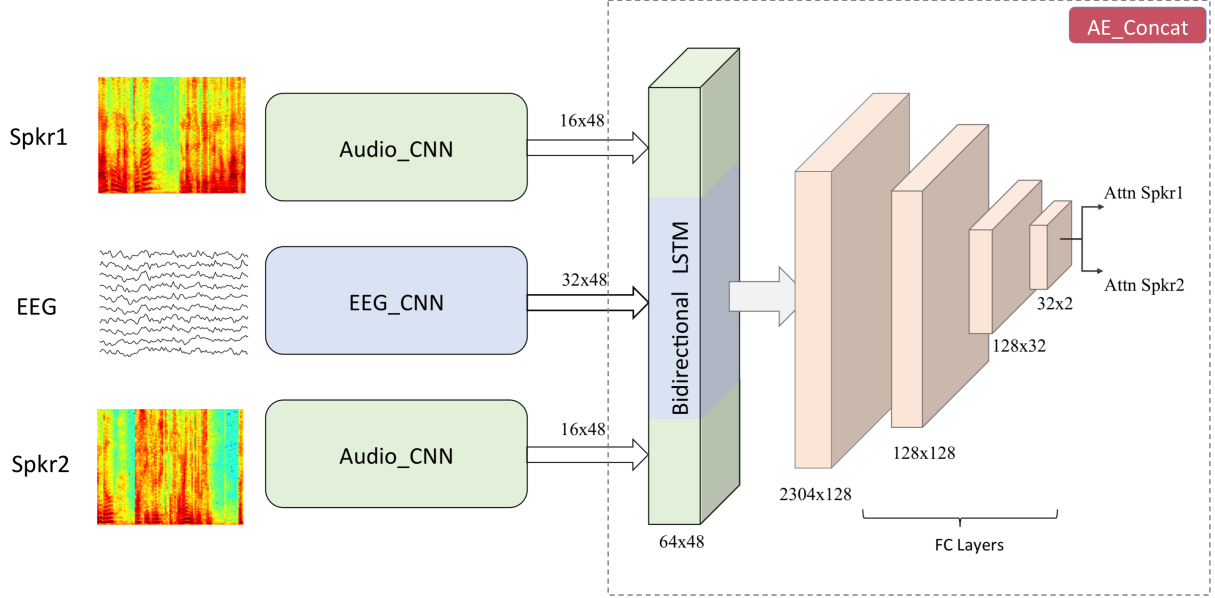


Fig. 1: The architecture of the proposed joint CNN-LSTM model. Input to the audio stream is the spectrogram of speech signals and input to the EEG stream is the downsampled version of EEG signals. Number of Audio_CNNs depends on the number of speakers present in the auditory scene (here two). From the outputs of Audio_CNN and EEG_CNN, speech and EEG embeddings are created which are concatenated together and passed to a BLSTM layer followed by FC layers.

B. Audio_CNN

The audio subnetwork that processed the speech spectrogram consisted of five convolution layers whose parameters are shown in Table IV. All standard procedures such as max pooling, batch normalization, dropout and ReLU activation were applied to the convolution output. Similar to the EEG_CNN, dimension of the input to the Audio_CNN varied according to the trial duration (Table II) but the dimension of the output feature map was always fixed at 48x16. As the datasets considered in this study were taken from dual-speaker experiments, the Audio_CNN was run twice resulting in two sets of output.

C. AE_Concat

The feature maps obtained from EEG_CNN and Audio_CNN were concatenated along the temporal axis and the dimension of the feature map after concatenation was 48x64. In this way, we ensured that half of the feature map was contributed from the EEG data and half of the feature map was contributed from the speech data. This also provides the flexibility to extend to more than two speakers such as the experiment performed in [35]. The concatenated feature map was passed through a bidirectional long short-term memory (BLSTM) layer [36] [37] which was followed by four fully connected (FC) layers. For the first three FC layers, ReLU activation was used and for the last FC layer, sigmoid activation was applied which helps us to classify the attention to speaker 1 or speaker 2. If more than two speakers are present, sigmoid activation should be replaced by softmax activation.

The total number of EEG samples and audio samples (trials) available was 118922 and 75% of the total available samples

(89192) were used to train the network and the rest of the available samples (29730) were equally split as validation and test data. The network was trained for 80 epochs using a mini batch size of 32 samples and with a learning rate of $5 * 10^{-4}$. The drop out probability was set to 0.25 for the EEG_CNN and the AE_Concat subnetworks but it was increased to 0.4 for the Audio_CNN subnetwork. A larger drop out probability was used for the Audio_CNN because speech stimuli were identical across subjects for a particular dataset. Hence, when trained on data from multiple subjects, the speech data remain identical and the network may remember the speech spectrogram of the training data. The network was optimized using Adam optimizer [38] and the loss function used was binary cross entropy. As neural network training can result in random variations from epoch to epoch, the test accuracy was calculated as the median accuracy of the last five epochs [39]. The network was trained using an Nvidia Geforce RTX-2060 (6 GB) graphics card and took approximately 36 hours to complete the training. The neural network model was developed in PyTorch and the python code is available at https://github.com/ivine-GIT/joint_CNN_LSTM_AAD.

D. Sparse Neural Network: Magnitude pruning

Although neural networks achieve state-of-the-art performances for a wide range of applications such as in the field of computer vision and natural language processing, they have large memory footprint and require extremely high computation power. Over the years, neural networks were able to extend their scope of applications by scaling up the network size. In 1998, the CNN model (LeNet) that was successful in recognizing handwritten digits consisted of under

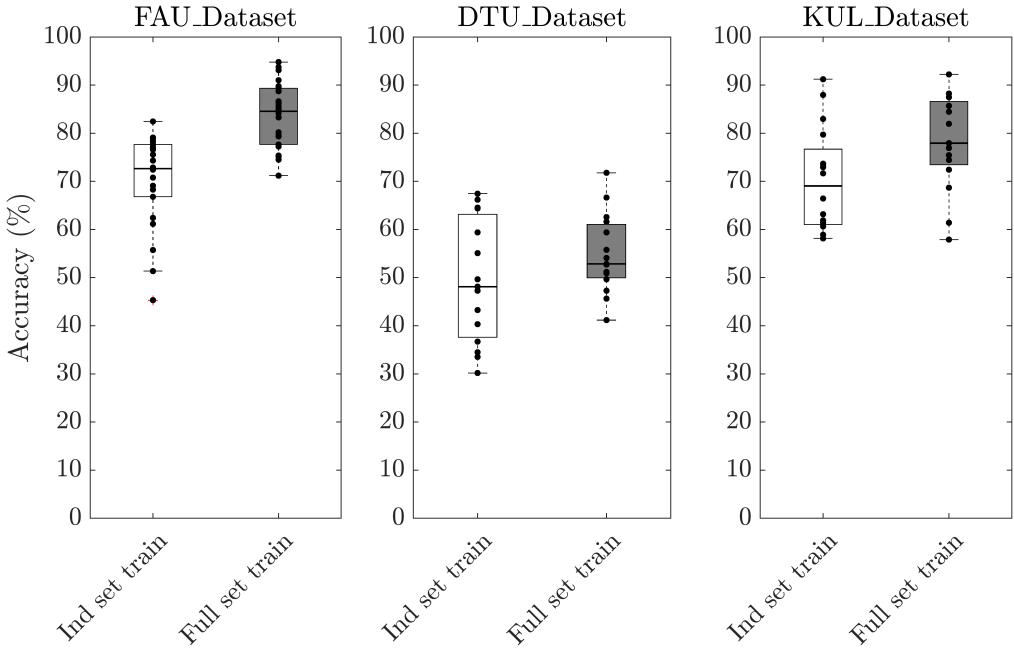


Fig. 2: Boxplot depicting the decoding accuracies obtained using two different training scenarios. In the first scenario (*Ind set train*), individual dataset accuracies were obtained by using training samples only from that particular dataset. For e.g., to calculate the test accuracy of FAU_Dataset, training samples were taken only from FAU_Dataset. In the second scenario (*Full set train*), individual dataset accuracies were obtained using training samples from all the three datasets combined. As a result, there are more training samples in the second scenario compared to the first.

a million parameters [40] whereas AlexNet that won the ImageNet challenge in 2012 consisted of 60 million parameters [41]. Neural networks were further scaled up to the order of 10 billion parameters and efficient methods to train these extremely large networks were presented in [42]. While these large models are very powerful, running them on embedded devices poses huge challenges due to the large memory and computation requirements. Sparse neural networks have been recently proposed to overcome these challenges and enable running these models on embedded devices [43]. In sparse networks, majority of the model parameters are zeros and zero-valued multiplications can be ignored thereby reducing the computational requirement. Similarly, only non-zero weights need to be stored on the device and for all the zero-valued weights, only their position needs to be known reducing the memory footprint. Empirical evidences have shown that neural networks tolerate high level of sparsity [43] [44] [45].

Sparse neural networks are found out by using a procedure known as network pruning. It consists of three steps. First, a large over-parameterized network is trained in order to obtain a high test accuracy as over-parameterization have stronger representation power [46]. Second, from the trained over-parametrized network, only important weights based on certain criterion are retained and all other weights are assumed to be redundant and reinitialized to zero. Finally, the pruned network is fine-tuned by training it further using only the retained weights so as to improve the performance. Searching for the redundant weights can be based on simple criteria such as magnitude pruning [43] or based on complex algorithms

such as variational dropout [47] or L0 regularization [48]. However, it was shown that introducing sparsity using magnitude pruning could achieve comparable or better performance than complex techniques such as variational dropout or L0 regularization [49]. Hence, we will present results based on only magnitude pruning in this work.

Sparsification of neural network has also been investigated as a neural network architecture search rather than merely as an optimization procedure. In the lottery ticket hypothesis presented in [50], authors posit that, inside the structure of an over-parameterized network, there exist subnetworks (winning tickets) that when trained in isolation reaches accuracies comparable to the original network. The pre-requisite to achieve comparable accuracy is to initialize the sparse network using the original random weight initialization that was used to obtain the sparse architecture. However, it was shown that with careful choice of the learning rate, the stringent requirement on original weight initialization can be foregone and the sparse network can be trained from scratch for any random initialization [51].

IV. RESULTS

A. Attention Decoding Accuracy

To evaluate how the proposed neural network model performs on different datasets, we trained our model under two different scenarios using a trial duration of 3 seconds. In the first scenario (*Ind set train*), attention decoding accuracies were calculated per individual dataset. I.e., to obtain the test

accuracy of subjects belonging to FAU_Dataset, the model was trained using training samples only from FAU_Dataset leaving out DTU_dataset and KUL_Dataset. Similarly, to obtain the test accuracy for DTU_Dataset, the model was trained using training samples only from DTU_Dataset. The same procedure was repeated for KUL_Dataset. The median decoding accuracy was 72.6% for FAU_Dataset, 48.1% for DTU_Dataset and 69.1% for KUL_Dataset (Fig. 2). In the second scenario (*Full set train*), accuracies were calculated by combining training samples from all the three datasets together. The median decoding accuracies obtained in this scenario were 84.5%, 52.9% and 77.9% for FAU_Dataset, DTU_Dataset and KUL_Dataset respectively. The results from the second scenario showed a clear improvement over the first scenario ($p < 0.001$) suggesting that the model generalizes better in the second scenario. Hence, all results presented further are based on training using samples combined from all the three datasets. Statistical analyses presented in this paper are based on paired Wilcoxon signed-rank test.

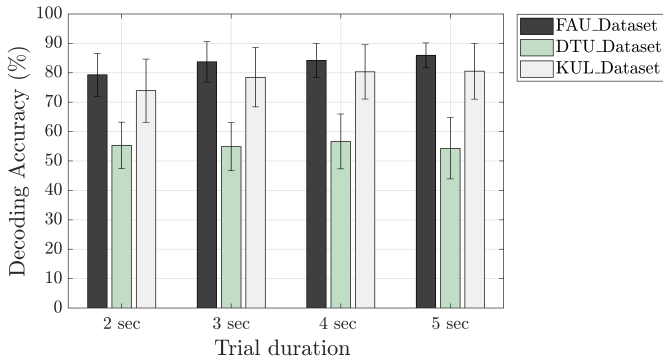


Fig. 3: Comparison of the decoding accuracies calculated for different trial durations per dataset.

B. Decoding Accuracy vs Trial Duration

To analyse the effect of trial duration on the attention decoding accuracy, the model was trained using trials of length 2, 3, 4 and 5 seconds. For every trial, only one second of new data were added and the remaining data were populated by overlapping to the previous trial using a sliding window. I.e., for 2 seconds trial, one second of overlap was used and for 3 seconds trial, two seconds of overlap was used and so on. In this way, total number of training samples remained constant for different trial durations considered in our analysis. The mean decoding accuracy across all subjects and datasets in case of 2 seconds trial duration was $70.9\% \pm 13.2\%$. The mean accuracy improved to $73.9\% \pm 14.8\%$ when the trial duration was increased to 3 seconds ($p < 0.001$). Using a trial duration of 4 seconds, the mean accuracy obtained was $75.2\% \pm 14.3\%$ which is a slight improvement with respect to the 3 seconds trials ($p < 0.05$). For 5 seconds trials, our neural network model resulted in a mean accuracy of $75.5\% \pm 15.7\%$ and was statistically identical to the accuracy obtained using 4 seconds trials ($p > 0.05$). Figure 3 depicts the accuracy calculated for individual datasets.

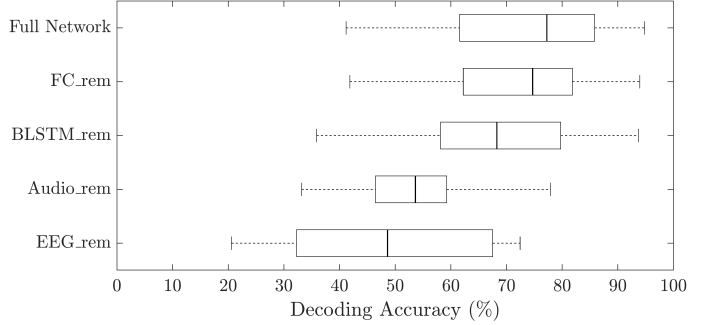


Fig. 4: Boxplots showing the decoding accuracies obtained by ablating the different blocks such as FC layer or BLSTM layer. To obtain the test accuracies after ablating, the ablated network was trained from scratch in case of FC_rem and BLSTM_rem. However, in case of Audio_rem and EEG_rem, accuracies were calculated by zeroing out the corresponding input features before passing them to a fully trained network.

C. Ablation Analysis

In order to gain further insights into the architecture of the neural network and understand the contribution of different parts of the model, we performed ablation analysis. I.e., we modified the neural network architecture by removing specific block such as the BLSTM layer or the FC layers one at a time and retrained the modified network. Similarly, to understand the importance of the audio input feature, decoding accuracies were calculated by zeroing out the EEG input and to understand the importance of the EEG input feature, decoding accuracies were calculated by zeroing out the audio input. The median decoding accuracy by zeroing out the EEG input was 48.6% whereas zeroing out the audio input resulted in an accuracy of 53.6% (Fig. 4). When the network was retrained by removing the BLSTM layer only, the median decoding accuracy obtained was 68.3% and on removing the FC layers only, median decoding accuracy was 74.7%. To compare, the median decoding accuracy calculated using the full the network was 77.2%.

D. Sparse Neural Network using Magnitude Pruning

To investigate the degree of sparsity that our neural network can tolerate, we pruned our network at 40%, 50%, 60%, 70% and 80% sparsity. In order to fine-tune the pruned neural network, there are two options: 1) sequential or 2) one-shot. In sequential fine-tuning, weights of the trained original model are reinitialized to zero in smaller steps per epoch until the required sparsity is attained. In one-shot fine-tuning, weights of the trained original model are reinitialized to zero at one shot in the first epoch and the sparse model is further trained to improve performance. We observed that the sequential fine-tuning is less efficient than one-shot fine-tuning in terms of training time budget. Therefore, all results presented here are based on one-shot method. We achieved a median decoding accuracy of 76.9% at a sparsity of 40% which is statistically identical to the original model at 77.2% ($p > 0.05$). When the sparsity was increased to 50%, the median decoding accuracy

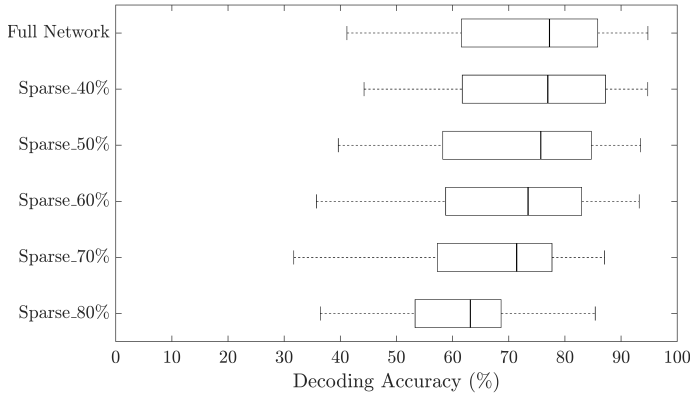


Fig. 5: Plots comparing the trade off between decoding accuracies and sparsity levels.

decreased to 75.7% which was lower than the original model ($p < 0.001$). Increasing the sparsity level further resulted in deterioration of decoding accuracy reaching 63.2% at a sparsity of 80% (Fig. 5). Total number of learnable parameters in our model was 416741 and to find the sparse network, we pruned only the weights leaving the bias and BN parameters unchanged. We additionally investigated the lottery ticket hypothesis [50] and training the sparse network from scratch [51] using a 50% sparse model and both algorithms yielded accuracies lower than chance level.

V. DISCUSSION

People with hearing loss suffer from deteriorated speech intelligibility in noisy acoustic environment such as multi-speaker scenario. Increasing the audibility by means of hearing aids have not shown to provide sufficient improvement to the speech intelligibility as hearing aids are unable to estimate *a priori* to which speaker the user intends to listen. Hence, hearing aids amplify both the wanted signal (attended speaker) and interfering signals (ignored speakers). Recently, it has been shown that the cortical signals measured using EEG could infer the auditory attention by discriminating between the attended speaker and the ignored speaker in a dual-speaker scenario [7]. Linear system analysis has been the commonly used methodology to analyse the EEG signals measured from a listener performing selective attention in a multi-speaker scenario. However, in recent years, non-linear analyses based on neural networks have become prominent, thanks to the availability of customized hardware accelerators and associated software libraries.

In this work, we developed a joint CNN-LSTM model to infer the auditory attention of a listener in a multi-speaker environment. CNNs take the EEG signal and spectrogram of the multiple speakers as inputs and extract features through successive convolutions. These convolutions generate an intermediate embeddings of the inputs which are then given to a BLSTM layer. As LSTMs fall under the category of recurrent neural networks, they can model the temporal relationship between the EEG embedding and the multiple spectrogram embeddings. Finally, the output of the BLSTM is processed

through FC layers to infer the auditory attention. The effectiveness of the proposed neural network was evaluated with the help of three different EEG datasets collected from subjects who undertook dual-speaker experiment.

A. Attention Decoding Accuracy

We analysed the performance of our neural network in two different training scenarios. In the first scenario, individual dataset accuracy was found out by training the network using samples taken only from that particular dataset. On the other hand, in the second scenario, individual dataset accuracy was found out by training using samples combined from all three datasets together. The accuracies obtained in the second scenario were higher than the first scenario by 10.8% on average which is in agreement with the postulate of neural network learning that larger the amount of training data, better the generalization. The decoding accuracies obtained for subjects belonging to the DTU_Dataset were markedly lower than the other two datasets similar to the observation made in [52]. While the exact reason for the lower performance is unclear, a major difference of the DTU_Dataset compared to the other two datasets was that the former consisted of attention to male and female speakers whereas the latter consisted of attention to only male speakers. Therefore, training with additional EEG data that consist of attention to female speakers can provide more insights into the lower performance.

B. Decoding Accuracy vs Trial Duration

One of the major challenges that AAD algorithms based on linear system theory faces is the deteriorated decoding performance when the trial duration is reduced. To this end, we calculated the accuracies using our neural network for different trial durations of 2 seconds, 3 seconds, 4 seconds and 5 seconds. We observed a clear performance improvement when trial duration was increased from two to three seconds whereas for all other trial durations, accuracies did not improve substantially (Fig. 3). However, increasing the trial duration will result in larger latency needed to infer the auditory attention that can adversely affect applications which require real-time operation. Hence, three seconds trial duration may be an optimal operation point as it is known from a previous study that human brain tracks the sentence phrases and phrases are normally not longer than three seconds [53]. Similarly, our analysis made use of 10 electrodes distributed all over the scalp but future work should investigate the effect of reducing the number of electrodes so that algorithms based on neural networks can be integrated into devices such as hearing aids. We anticipate that the current network will require modifications with additional hyperparameter tuning in order to accommodate for the reduction in number of electrodes as fewer the number of electrode, lower is the amount of training data available.

C. Ablation Analysis

Performing ablation analysis gives the possibility to evaluate the contribution of different inputs and modules in a neural

network. To our model, when only the speech features were given as input, the median decoding accuracy was 48.6% whereas only EEG features as input resulted in an accuracy of 53.6% (Fig. 4). I.e., our neural network model learned more from the EEG features compared to the speech features. This is not surprising because in all the datasets that we analysed, speech stimuli were repeated across subjects while the EEG measured were unique. This also suggests that in future, care must be taken to design the experiment in such a way as to incorporate diverse speech stimuli. Further analysis ablating the BLSTM layer and the FC layers revealed that the BLSTM layer was far more important than the FC layers. This is probably due to the ability of the LSTM layer to model the temporal delay between speech cues and the EEG. However, we anticipate that when the training datasets become larger are more diverse, FC layers will grow in importance due to the improved representation and optimization power of dense networks [46].

D. Sparse Neural Networks

Investigation into the amount of sparsity that our neural network can tolerate revealed a tolerance of upto 50% sparsity without substantial loss of accuracy (Fig. 5). However, standard benchmarking on sparsity has found that deep networks such as ResNet-50 can tolerate upto 90% sparsity [49]. One of the potential reasons for the lower level of sparsity in our model is due to its shallow nature. I.e., our model is comprised of less than half a million learnable parameters while deep networks such as ResNet-50 is comprised of over 25 million learnable parameters. It is also interesting to note that the accuracy obtained by removing the FC layer in our ablation analysis was 74.6% compared to the full network accuracy of 77.2%. And the ablated network consisted of 105605 parameters which is approximately only a quarter of the total number of parameters (416741) of the original network. This shows that by careful design choices, we can reduce the network size considerably compared to an automatic sparse network search using magnitude pruning.

VI. CONCLUSION

Integrating EEG to track the cortical signals is one of the latest proposals to enhance the quality of service provided by hearing aids to the users. EEG is envisaged to provide neuro-feedback about the user's intention thereby enabling the hearing aid to infer and enhance the attended speech signals. In the present study, we propose a joint CNN-LSTM network to classify the attended speaker and subsequently infer the auditory attention of a listener. The proposed neural network uses speech spectrograms and EEG signals as inputs to infer the auditory attention. Results obtained by training the network using three different EEG datasets collected from multiple subjects who undertook a dual-speaker experiment showed that our network generalizes well to different scenarios. Investigation into the importance of different constituents of our network architecture revealed that adding an LSTM layer improved the performance of the model considerably. Evaluating sparsity on the proposed joint CNN-LSTM network demonstrates that the

network can tolerate upto 50% sparsity without considerable deterioration in performance. These results could pave way to integrate algorithms based on neural networks into hearing aids that have constrained memory and computational power.

ACKNOWLEDGMENT

This work was supported by a grant from *Johannes und Frieda Marohn-Stiftung, Erlangen*. We convey our gratitude to all participants who took part in the study and would like to thank the student Laura Rupprecht who helped us with data acquisition.

REFERENCES

- [1] E. C. Cherry, "Some experiments on the recognition of speech, with one and with two ears," *The Journal of the acoustical society of America*, vol. 25, no. 5, pp. 975–979, 1953.
- [2] J. Feldman, "What is a visual object?" *Trends in Cognitive Sciences*, vol. 7, no. 6, pp. 252–256, 2003.
- [3] B. G. Shinn-Cunningham, "Object-based auditory and visual attention," *Trends in cognitive sciences*, vol. 12, no. 5, pp. 182–186, 2008.
- [4] E. K. Vogel, G. F. Woodman, and S. J. Luck, "Pushing around the Locus of Selection: Evidence for the Flexible-selection Hypothesis," *Journal of Cognitive Neuroscience*, vol. 17, no. 12, pp. 1907–1922, 2005.
- [5] N. Mesgarani and E. F. Chang, "Selective cortical representation of attended speaker in multi-talker speech perception," *Nature*, vol. 485, no. 7397, pp. 233–236, 2012.
- [6] N. Ding and J. Z. Simon, "Neural coding of continuous speech in auditory cortex during monaural and dichotic listening," *Journal of Neurophysiology*, vol. 107, no. 1, pp. 78–89, 2012.
- [7] J. A. O'Sullivan, A. J. Power, N. Mesgarani, S. Rajaram, J. J. Foxe, B. G. Shinn-Cunningham, M. Slaney, S. A. Shamma, and E. C. Lalor, "Attentional Selection in a Cocktail Party Environment can be Decoded from Single-Trial EEG," *Cerebral Cortex*, vol. 25, no. 7, pp. 1697–1706, 2014.
- [8] S. J. Aiken and T. W. Picton, "Human Cortical Responses to the Speech Envelope," *Ear and hearing*, vol. 29, no. 2, pp. 139–157, 2008.
- [9] E. C. Lalor and J. J. Foxe, "Neural responses to uninterrupted natural speech can be extracted with precise temporal resolution," *European Journal of Neuroscience*, vol. 31, no. 1, pp. 189–193, 2010.
- [10] G. M. Di Liberto, J. A. O'Sullivan, and E. C. Lalor, "Low-Frequency Cortical Entrainment to Speech Reflects Phoneme-Level Processing," *Current Biology*, vol. 25, no. 19, pp. 2457–2465, 2015.
- [11] M. P. Broderick, A. J. Anderson, and E. C. Lalor, "Semantic Context Enhances the Early Auditory Encoding of Natural Speech," *Journal of Neuroscience*, vol. 39, no. 38, pp. 7564–7575, 2019.
- [12] L. Fiedler, M. Woestmann, C. Graversen, A. Brandmeyer, T. Lunner, and J. Obleser, "Single-channel in-ear-EEG detects the focus of auditory attention to concurrent tone streams and mixed speech," *Journal of Neural Engineering*, vol. 14, no. 3, p. 036020, 2017.
- [13] I. Kuruvila, E. Fischer, and U. Hoppe, "An LMMSE-based Estimation of Temporal Response Function in Auditory Attention Decoding," in *2020 42nd Annual International Conference of the IEEE Engineering in Medicine & Biology Society (EMBC)*. IEEE, 2020, pp. 2837–2840.
- [14] W. Biesmans, N. Das, T. Francart, and A. Bertrand, "Auditory-Inspired Speech Envelope Extraction Methods for Improved EEG-Based Auditory Attention Detection in a Cocktail Party Scenario," *IEEE Transactions on Neural Systems and Rehabilitation Engineering*, vol. 25, no. 5, pp. 402–412, 2017.
- [15] B. Mirkovic, S. Debener, M. Jaeger, and M. De Vos, "Decoding the attended speech stream with multi-channel EEG: implications for online, daily-life applications," *Journal of Neural Engineering*, vol. 12, no. 4, p. 046007, 2015.
- [16] L. Fiedler, M. Wöstmann, S. K. Herbst, and J. Obleser, "Late cortical tracking of ignored speech facilitates neural selectivity in acoustically challenging conditions," *NeuroImage*, vol. 186, pp. 33–42, 2019.
- [17] I. Kuruvila, K. C. Demir, E. Fischer, and U. Hoppe, "Inference of the Selective Auditory Attention using Sequential LMMSE Estimation," *arXiv preprint arXiv:2102.01746*, 2021.
- [18] E. Zwicker and H. Fastl, *Psychoacoustics: Facts and models*. Springer Science & Business Media, 2013, vol. 22.

[19] S. A. Fuglsang, T. Dau, and J. Hjortkjær, "Noise-robust cortical tracking of attended speech in real-world acoustic scenes," *NeuroImage*, vol. 156, pp. 435–444, 2017.

[20] S. Geirnaert, T. Francart, and A. Bertrand, "An Interpretable Performance Metric for Auditory Attention Decoding Algorithms in a Context of Neuro-Steered Gain Control," *IEEE Transactions on Neural Systems and Rehabilitation Engineering*, vol. 28, no. 1, pp. 307–317, 2019.

[21] S. Miran, S. Akram, A. Sheikhattar, J. Z. Simon, T. Zhang, and B. Babadi, "Real-Time Tracking of Selective Auditory Attention From M/EEG: A Bayesian Filtering Approach," *Frontiers in Neuroscience*, vol. 12, p. 262, 2018.

[22] A. Craik, Y. He, and J. L. Contreras-Vidal, "Deep learning for electroencephalogram (EEG) classification tasks: a review," *Journal of Neural Engineering*, vol. 16, no. 3, p. 031001, 2019.

[23] T. de TAILLEZ, B. KOLLMEIER, and B. T. MEYER, "Machine learning for decoding listeners' attention from electroencephalography evoked by continuous speech," *European Journal of Neuroscience*, vol. 51, no. 5, pp. 1234–1241, 2020.

[24] G. Ciccarelli, M. Nolan, J. Perricone, P. T. Calamia, S. Haro, J. O'Sullivan, N. Mesgarani, T. F. Quatieri, and C. J. Smalt, "Comparison of two-talker attention decoding from EEG with nonlinear neural networks and linear methods," *Scientific reports*, vol. 9, no. 1, pp. 1–10, 2019.

[25] L. Deckers, N. Das, A. H. Ansari, A. Bertrand, and T. Francart, "EEG-based detection of the attended speaker and the locus of auditory attention with convolutional neural networks," *bioRxiv*.

[26] M. J. Monesi, B. Accou, J. Montoya-Martinez, T. Francart, and H. Van Hamme, "An LSTM Based Architecture to Relate Speech Stimulus to Eeg," in *ICASSP 2020-2020 IEEE International Conference on Acoustics, Speech and Signal Processing (ICASSP)*. IEEE, 2020, pp. 941–945.

[27] Tian, Yin and Ma, Liang, "Auditory attention tracking states in a cocktail party environment can be decoded by deep convolutional neural networks," *Journal of Neural Engineering*, 2020.

[28] D. Wang and J. Chen, "Supervised Speech Separation Based on Deep Learning: An Overview," *IEEE/ACM Transactions on Audio, Speech, and Language Processing*, vol. 26, no. 10, pp. 1702–1726, 2018.

[29] A. Ephrat, I. Mosseri, O. Lang, T. Dekel, K. Wilson, A. Hassidim, W. T. Freeman, and M. Rubinstein, "Looking to listen at the cocktail party: A speaker-independent audio-visual model for speech separation," *arXiv preprint arXiv:1804.03619*, 2018.

[30] S. A. Fuglsang, D. D. Wong, and J. Hjortkjær, "EEG and audio dataset for auditory attention decoding," 2018. [Online]. Available: <https://doi.org/10.5281/zenodo.1199011>

[31] N. Das, T. Francart, and A. Bertrand, "Auditory Attention Detection Dataset KULEuven," 2019. [Online]. Available: <https://doi.org/10.5281/zenodo.3377911>

[32] N. Das, W. Biesmans, A. Bertrand, and T. Francart, "The effect of head-related filtering and ear-specific decoding bias on auditory attention detection," *Journal of Neural Engineering*, vol. 13, no. 5, p. 056014, 2016.

[33] N. Srivastava, G. Hinton, A. Krizhevsky, I. Sutskever, and R. Salakhutdinov, "Dropout: a simple way to prevent neural networks from overfitting," *Journal of Machine Learning Research*, vol. 15, no. 1, pp. 1929–1958, 2014.

[34] S. Ioffe and C. Szegedy, "Batch normalization: Accelerating deep network training by reducing internal covariate shift," *arXiv preprint arXiv:1502.03167*, 2015.

[35] P. J. Schäfer, F. I. Corona-Strauss, R. Hannemann, S. A. Hillyard, and D. J. Strauss, "Testing the Limits of the Stimulus Reconstruction Approach: Auditory Attention Decoding in a Four-Speaker Free Field Environment," *Trends in Hearing*, vol. 22, p. 2331216518816600, 2018.

[36] S. Hochreiter and J. Schmidhuber, "Long short-term memory," *Neural computation*, vol. 9, no. 8, pp. 1735–1780, 1997.

[37] M. Schuster and K. K. Paliwal, "Bidirectional recurrent neural networks," *IEEE transactions on Signal Processing*, vol. 45, no. 11, pp. 2673–2681, 1997.

[38] D. P. Kingma and J. Ba, "Adam: A method for stochastic optimization," *arXiv preprint arXiv:1412.6980*, 2014.

[39] P. Goyal, P. Dollár, R. Girshick, P. Noordhuis, L. Wesolowski, A. Kyrola, A. Tulloch, Y. Jia, and K. He, "Accurate, large minibatch sgd: Training imagenet in 1 hour," *arXiv preprint arXiv:1706.02677*, 2017.

[40] Y. LeCun, L. Bottou, Y. Bengio, and P. Haffner, "Gradient-Based Learning Applied to Document Recognition," *Proceedings of the IEEE*, vol. 86, no. 11, pp. 2278–2324, 1998.

[41] A. Krizhevsky, I. Sutskever, and G. E. Hinton, "ImageNet Classification with Deep Convolutional Neural Networks," *Communications of the ACM*, vol. 60, no. 6, pp. 84–90, 2017.

[42] A. Coates, B. Huval, T. Wang, D. Wu, B. Catanzaro, and N. Andrew, "Deep learning with cots hpc systems," in *International conference on machine learning*. PMLR, 2013, pp. 1337–1345.

[43] S. Han, J. Pool, J. Tran, and W. Dally, "Learning both Weights and Connections for Efficient Neural Network," *Advances in Neural Information Processing Systems*, vol. 28, pp. 1135–1143, 2015.

[44] S. Narang, E. Elsen, G. Diamos, and S. Sengupta, "Exploring Sparsity in Recurrent Neural Networks," *arXiv preprint arXiv:1704.05119*, 2017.

[45] M. Zhu and S. Gupta, "To prune, or not to prune: exploring the efficacy of pruning for model compression," *arXiv preprint arXiv:1710.01878*, 2017.

[46] J.-H. Luo, J. Wu, and W. Lin, "Thinet: A filter level pruning method for deep neural network compression," in *Proceedings of the IEEE international conference on computer vision*, 2017, pp. 5058–5066.

[47] D. Molchanov, A. Ashukha, and D. Vetrov, "Variational Dropout Sparsifies Deep Neural Networks," *arXiv preprint arXiv:1701.05369*, 2017.

[48] C. Louizos, M. Welling, and D. P. Kingma, "Learning Sparse Neural Networks through L_0 Regularization," *arXiv preprint arXiv:1712.01312*, 2017.

[49] T. Gale, E. Elsen, and S. Hooker, "The State of Sparsity in Deep Neural Networks," *arXiv preprint arXiv:1902.09574*, 2019.

[50] J. Frankle and M. Carbin, "The Lottery Ticket Hypothesis: Finding Sparse, Trainable Neural Networks," *arXiv preprint arXiv:1803.03635*, 2018.

[51] Z. Liu, M. Sun, T. Zhou, G. Huang, and T. Darrell, "Rethinking the Value of Network Pruning," *arXiv preprint arXiv:1810.05270*, 2018.

[52] S. Geirnaert, S. Vandecappelle, E. Alickovic, A. de Cheveigné, E. Lalor, B. T. Meyer, S. Miran, T. Francart, and A. Bertrand, "Neuro-Steered Hearing Devices: Decoding Auditory Attention From the Brain," *arXiv preprint arXiv:2008.04569*, 2020.

[53] M. Vander Ghinst, M. Bourguignon, M. Niesen, V. Wens, S. Hassid, G. Choufani, V. Jousmäki, R. Hari, S. Goldman, and X. De Tiège, "Cortical tracking of speech-in-noise develops from childhood to adulthood," *Journal of Neuroscience*, vol. 39, no. 15, pp. 2938–2950, 2019.